Image processing of electron micrographs of human alpha2-macroglobulin half-molecules induced by Cd2+

ARTICLE *in* BIOLOGY OF THE CELL · FEBRUARY 1988

Impact Factor: 3.51 · DOI: 10.1016/0248-4900(88)90091-3 · Source: PubMed

Biology of the Cell, 64 (1988) 39–44

Original article

Image processing of electron micrographs of human alpha$_2$-macroglobulin half-molecules induced by Cd^{2+}

Daniel THOMAS[1] *, Mohamed J. FLIFLA[2], Brigitte ESCOFFIER[3], Martine BARRAY[4] and Etienne DELAIN[4]

[1] *Laboratoire de Biologie Cellulaire, UA 256 CNRS;*
[2] *Laboratoire de Traitement du Signal;*
[3] *IRISA (INRIA-CNRS), Université de Rennes 1, Campus de Beaulieu, 35040 Rennes Cedex; and*
[4] *Laboratoire de Microscopie Cellulaire et Moléculaire, UA 147 CNRS, Institut Gustave-Roussy, rue Camille-Desmoulins, 94805 Villejuif Cedex, France*

(Received 22-2-1988; accepted 24-6-1988)

Human alpha$_2$-macroglobulin is a tetrameric plasma inhibitor of proteinases. Its dissociation by Cd^{2+} gives functional dimers. Electron microscopy of negatively stained dimers shows their round-ended cylindrical shape with furrows delimiting 3 main stain-excluding domains. Image processing of electron micrographs shows the existence of 2 main orientations of the dimers on the carbon support film. The dimer is composed of 2 curved monomers linked in a central domain, and related by a 90° rotation. Taking into account the known primary structure of alpha$_2$-macroglobulin and the linkage of the 2 constitutive monomers by 2 disulfide bonds, the molecular organization of the dimer is discussed, extended to the tetrameric molecule and compared to the published models of human alpha$_2$-macroglobulin.

α_2-macroglobulin — correspondence analysis — image processing — electron microscopy

INTRODUCTION

Alpha$_2$-macroglobulin (α_2M) is a tetrameric plasma glycoprotein (720 kD), which can undergo a considerable conformational change. This change is the result of the activation of internal thiolesters, either by the direct action of primary amines, or by proteolysis of the bait region present in each monomer [1, 15, 19, 22]. Electron microscopy has given clear ideas of the structure of the tetrameric proteinase-complexed α_2M as shaped like an H [2, 3, 13, 14, 17, 18]. The structure of the native α_2M tetramer remains, however, under discussion, as does the modeling of the observed structural changes of α_2M from the native to the transformed state [3, 5, 6, 12, 17]. The native tetrameric α_2M molecule can be easily dissociated by Cd^{2+} into halves, each comprising 2 disulfide-bound monomers [4], to make functional dimers or half-molecules [16]. Immunoelectron microscopy has revealed the location of various epitopes on dimeric and tetrameric native or chymotrypsin-complexed α_2M [5]. Structural implications have arisen from these results, leading to a new tentative model of native and transformed α_2M organization and conformational changes [5].

In order to understand better the unresolved structure of native human α_2M, we have investigated, by multivariate statistical analysis of electron micrographs, the molecular organization of the most simple Cd^{2+}-induced α_2M dimers. The results obtained here on dimers, and by immunoelectron microscopy on dimeric and tetrameric α_2M [5], have been used to propose a new interpretation of the native α_2M organization.

MATERIAL AND METHODS

α_2M dimers

Native tetrameric and Cd_{2+}-induced α_2M dimers were obtained as already described, by incubating for 30 min at 37°C native α_2M in 10mM $CdCl_2$ in 50mM Na cacodylate pH 7.2 [3, 16]. Dimers appear as a very homogeneous population, as seen in the electron microscope, and were used without further purification.

Electron microscopy

This was realized as previously described [18]. Dimers negatively stained with 2% aqueous uranyl acetate pH 4.5 were recorded at 80 kV with a Zeiss 902 electron microscope equipped with a liquid nitrogen anticontamination device. Optimal contrast was obtained by use of the electron energy loss spectrometer to eliminate the inelastically scattered electrons, in combination with a 30-μm objective aperture. The specimen grid was placed into the cartridge in such a way that the molecules were oriented facing the incident electron beam. The direct magnification was calibrated with the 2.3 nm transverse periodicity of the tobacco mosaic virus, mixed with the dimers.

* *Correspondence and reprints*

The quality and resolution of the negatives was assessed by optical diffraction, which reveals a continuous transfer interval up to 0.66 nm^{-1}, corresponding to a reliable resolution of 1.5 nm. After selection of a representative square on a grid, with many well contrasted dimers, only one negative was used in order to avoid dispersion in the images due to local variations in stain thickness. The micrograph (×32,000) was digitized with an Optronic rotating drum densitometer, with a raster step of 25 μm corresponding to 0.7 nm on the specimen scale. Each of the 5 digitized 512×512 images contained 20–30 dimers. Selection consisted of choosing isolated molecules, to avoid alignment problems with those too close to each other. Thus no *a priori* selection was done according to the shape of the molecules. The orientation of the negatives was maintained to keep the correct enantiomorphism of the molecules.

Image processing

General manipulations of the images were performed on an HP 9000 Computer using programs specially developed for this purpose, and on a VAX 11/750 using the PIC system [20]. For alignment we used alternating sequences of translational and rotational correlations of the images of the molecules [7]. A well preserved image was chosen as a reference, centered using the autocorrelation function (ACF), then used to align all images. After a first pass, the alignment was refined with, as a new reference, the average of the 10 molecules that showed the highest correlation with the former reference. In order to distinguish between positions related by 180° rotation in the image, a 180° rotational test was performed relative to the reference, using the correlation function. Of the 53 images used, 12 were rejected because they did not converge stably in correlation alignment. Correspondence analysis of molecule images was performed by means of the SPAD software developed by Lebart and Morineau [11]. Before the aligned images entered the correspondence analysis, they were low-pass filtered and surrounded by a narrow mask to restrict the analysis to the dimer itself and its surrounding stain layer. Such filtered images served only for statistical analysis; subsequent averaging of the subsets was done with the unfiltered aligned images [21].

The mask was realized on an averaged picture of 10 molecules. After thresholding, this picture was binarized and then subjected to a series of erosion and dilation operations.

To interpret the results of the correspondence analysis, we determined the meaning of each factor by examining importance images [9], and by averaging images that were lying close together on the factorial map. Finally, the resulting averaged images were band-limited between 0.3 and 0.6 nm^{-1}, the resolution limit was estimated by using the phase residual method as described by Frank *et al.* [8].

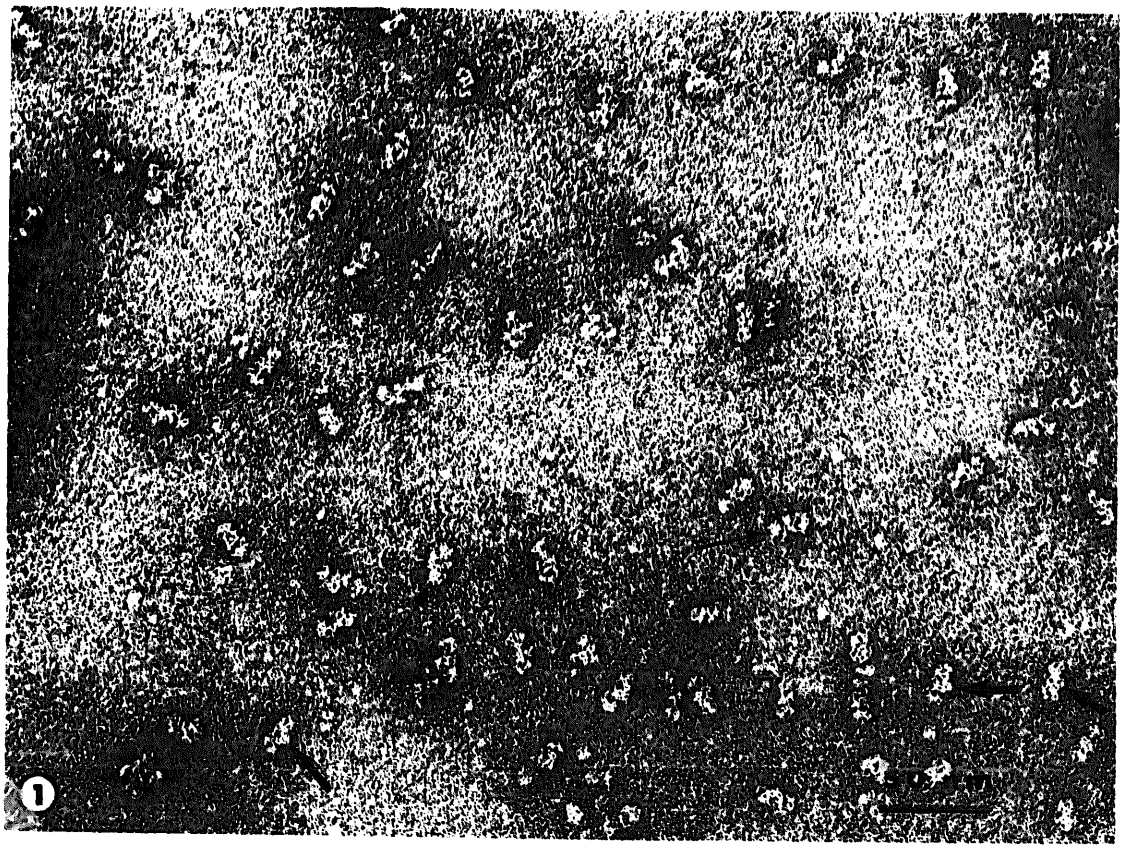

FIGURE 1. – Portion of an electron micrograph of α_2-M dimers, used in the analysis. The dimers are round-cnded cylinders (→). Some have a central, laterally protruding domain (➧). Bar, 50 nm.

RESULTS

Electron microscopy of α_2M dimers

A representative view of the molecules negatively stained with uranyl acetate is shown in Figure 1. Dimers are elongated particles $18.9 \pm 1.3 \times 8.7 \pm 0.2$ nm (64 measurements) with stain-filled furrows or small depressions, often giving a 3-nodular aspect to the particles. The central domain can protrude on one side (➧) or the molecule can appear like a round-ended cylinder (→).

Correspondence analysis of the images

The results of the correspondence analysis are shown on a map spanned by 2 factors in which each dot represents an image (Figure 2). Images having a close resemblance are positioned closely on the map. In our study, the first factor accounts for 21.6% of the total interimage variance, while factors 2, 3, and 4 account for only 9.5%, 7.6%, and 7.0%, respectively. Thus, the first factor corresponds to the most predominant differences present in the population images; along this axis (F1), images are clearly separated into 2 groups. The averaged images obtained from each cluster (Fig. 3 a,b and Fig. 3 c,d) clearly show that the molecules are divided along the first factor into 2 subpopulations according to significant morphological differences. The importance image, corresponding to this factor (Fig. 4a), indicates that the positions of the projections of the molecules along the first axis correspond to strong differences in the stain distribution at the periphery of the molecule due to shape differences. To determine the meaning of the second factor, both clusters were divided into 2 subclusters along this axis and images were averaged in each subcluster. Figures 3a,c, and Figures 3b,d correspond, respectively, to averaged images from the positive and the negative values along factor 2. These averages and the corresponding importance image (Fig. 4b) reveal that the second factor reflects small modifications of features defined by the stain accumulation (or stain exclusion) due to regional variation of peripheral staining.

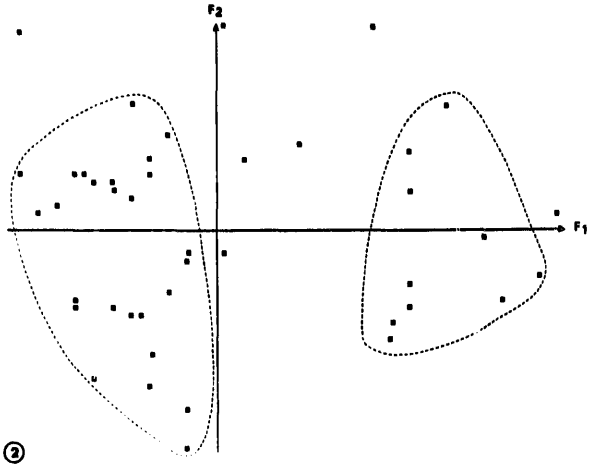

FIGURE 2. – Two-dimensional correspondence analysis map of α_2M dimers showing the first 2 factors. The first factor, which accounts for 21.6% of the total interimage variance, corresponds to predominant differences.

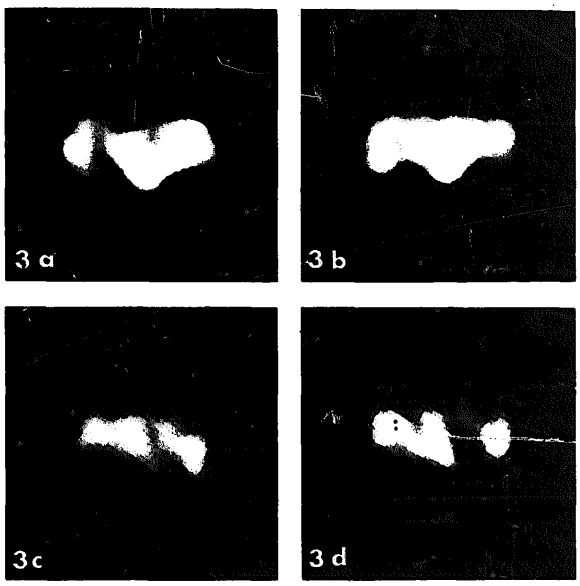

FIGURE 3. – To determine the meaning of each factor, images were averaged in each cluster. Figures 3a,b, and Figures 3c,d, correspond to the positive and the negative values along factor 1, respectively. Figures 3a,c, and Figures 3b,d, correspond to the positive and the negative values along factor 2, respectively.

Image interpretation

From these results it appears that only the first factor carries a meaningful discrimination in terms of the structure of the molecule. Averaged images obtained from the negative values ($N=26$) and from the positive values ($N=10$) of factor 1 correspond, respectively, to 2 projections of the dimer (Fig. 5). These images and the plasticine model show that the dimer consists of 3 stain-excluding domains. The largest, central one, is considered to correspond to the zone where the 2 monomers are joined. In Figure 5a,c,e the monomer on the left is lying on its side on the support film, while that on the right is facing down the film. In Figure 5b,d,f the subunit on the left is facing up, and that on the right is lying on its side. Both projections (a,c,e and b,d,f) could be related by a ≃ 90° rotation around the long axis, or by a flip of 180°. The monomer has a curved shape with a stain-excluding region at one extremity, the dimer being composed of 2 orthogonally related monomers linked in the middle in a high stain-excluding region.

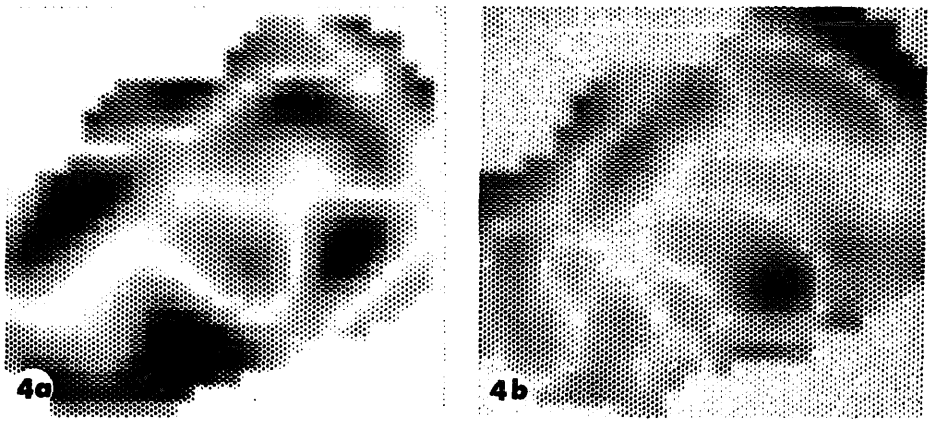

FIGURE 4. – Importance images of the first (a) and second (b) factors. This representation allows all pixels to be assessed for their relative importance in defining the associated data separation. A weight is attached to each pixel according to its position along the associated axis. Here, black areas indicate the pixels which give the largest contributions to the factor.

DISCUSSION

The complete sequence of human α_2M is known, as well as the location of the 2 disulfide bridges connecting the 2 antiparallel monomers near the *N*-terminal ends [10]. However, the 3-dimensional organization of native or transformed tetrameric α_2M remains under discussion, as several contradictory models have been proposed [3, 5, 6, 13, 17]. The large variability in the morphology of native α_2M observed in negative staining led us to analyze the organization of the half-molecules obtained by Cd^{2+} dissociation of native α_2M. The present study showed that these dimers are cylindrical structures with 2 rounded ends and perpendicularly oriented furrows. Immunoelectron microscopy has shown that various monoclonal antibodies (mAbs) bind to epitopes located at both extremities of the dimer, thus demonstrating the relative disposition of the disulfide-bound monomers in the Cd^{2+}-induced dimer. We have illustrated this observation in an interpreting model [5]. Different results are in favor of our hypothesis that the C-terminal end of each monomer is not accessible in the native form. First, biochemical and immunoelectron microscope data with mAbs specific for epitopes located on the 20 kD domain of α_2M revealed that these epitopes are not expressed (not present or not accessible) in the native form of dimeric or tetrameric α_2M [5, 24]. Second, the receptor-recognition site also located on this 20 kD domain is not expressed in native α_2M [23, 24]. And third, this 20 kD domain remains linked to the tetrameric native molecule even after proteolysis by a bacterial proteinase which is not inhibited by α_2M; hydrolysis of the thiolesters by methylamine or trypsin treatment, and the concomitant conformational change of the native α_2M are needed for the release of the 20 kD domain and for the expression of both the receptor-recognition site and the epitopes on the 20 kD-specific mAbs [24]. All these data indicate that these epitopes and the receptor-recognition site may be masked or buried in the native form, either dimeric or tetrameric, or appear as neo-antigens on the transformed α_2M after the profound reorganization induced by thiolester hydrolysis.

The present image analysis demonstrates the existence of 3 stain-excluding domains in the cylindrical round-ended dimer. The 2 extremities appear as curved structures related by an angle of about 90°, and connected in a central region forming the third stain-excluding domain. The general shape of the dimer appears as that of a dumpy, twisted letter S. With regard to the proposed organization of the dimer [10], *i.e.*, 2 identical antiparallel chains connected near their *N*-terminal ends by 2 disulfide bridges, we consider that the central region of the dimer corresponds to the 2 *N*-terminal domains with the 2 connecting disulfide bridges, whereas the 2 C-terminal segments make the 2 rounded ends.

Our hypothesis is that when the conformational change occurs, the 2 rounded ends unroll and expose the C-terminal portion of the dimer, thus expressing the receptor-recognition site and the epitopes of the mAbs specific for the 20 kD domain. This is documented by the structure of the chymotrypsin-transformed Cd^{2+}-induced dimer, which looks like a U, with half the size of an H-like transformed tetramer [5]. To go back to the whole native tetrameric α_2M molecule, it is tempting to consider it as a cross-like assembly of 2 dimers. Its various orientations, and the distortions induced by the deposition on a carbon film would explain the variable aspect of negatively stained human α_2M [3, 13, 14, 18]. It is interesting to note that a clear cross-like organization is usually found in ovomacroglobulins, which are homologs of α_2M [14]. A reexamination by image processing of the structure of native tetrameric human α_2M is currently in progress.

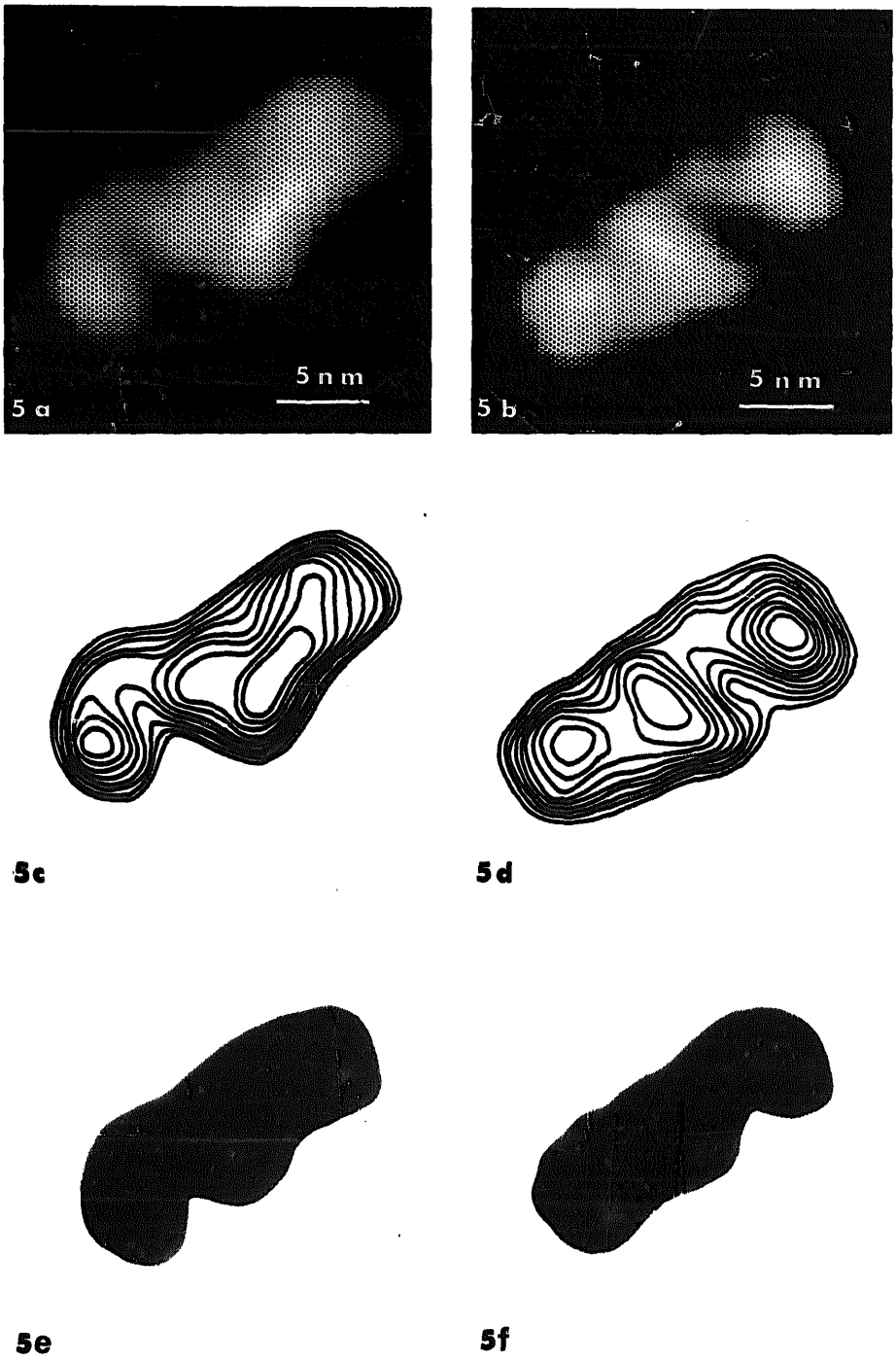

FIGURE 5. – Averaged images of the 2 projections of the α_2M dimer obtained from the negative values (**a** and **c**) ($n = 26$) and the positive values (**b** and **d**) ($n = 10$) of factor 1. (**a**) and (**b**) are density plots, (**c**) and (**d**) contour plots. Bar, 5 nm. (**e**) and (**f**) are photographs of the plasticine model and correspond to the 2 projections. The model is turned by 90° along its longitudinal axis to illustrate the 2 projections obtained by image processing.

ACKNOWLEDGEMENTS

Fred Van Leuven and François Pochon are thanked for helpful discussions. Dr. Claude Labit is acknowledged for facilities and help in computing, M. Mathelier for graphics, and L. Communier for photoprinting.

REFERENCES

1 Barrett A.J. (1981) α_2-Macroglobulin. *Methods Enzymol.* 80, 737–754
2 Bonnet N. & Delain E. (1985) Digital acquisition and processing of STEM images of α_2-macroglobulin complexed with proteinases or zinc. *J. Microsc. Spectrosc. Electron* 10, 505–514
3 Bretaudière J.-P., Tapon-Bretaudière J. & Stoops J.K. (1988) Structure of native α_2-macroglobulin and its transformation to the protease-bound form. *Proc. Natl. Acad. Sci. USA* 85, 1437–1441
4 Couture-Tosi E., Tapon-Bretaudière J., Pochon F., Barray M., Bros A. & Delain E. (1986) Ultrastructural and antiproteinase activity modifications of human α_2-macroglobulin induced by zinc and other divalent cations. *Eur. J. Cell Biol.* 42, 359–364
5 Delain E., Barray M., Tapon-Bretaudière J., Pochon F., Marynen P., Cassiman J.J., Van Den Berghe H. & Van Leuven F. (1988) The molecular organization of human α_2-macroglobulin: an immunoelectron microscopic study with monoclonal antibodies. *J. Biol. Chem.* 263, 2981–2989
6 Feldman S.R., Gonias S.L. & Pizzo S.V. (1985) Model of α_2-macroglobulin structure and functions. *Proc. Natl. Acad. Sci. USA* 82, 5700–5704
7 Frank J., Goldfarb W., Eisenberg D. & Baker T.S. (1978) Reconstruction of glutamine synthetase using computer averaging. *Ultramicroscopy* 3, 283–290
8 Frank J., Verschoor A. & Boublik M. (1981) Computer averaging of electron micrographs of 40 S ribosomal subunits. *Science* 214, 1353–1355
9 Frank J., Verschoor A. & Boublik M. (1982) Multivariate statistical analysis of ribosome electron micrographs. (L and R lateral views of the 40 S subunit from HeLa cells.) *J. Mol. Biol.* 161, 107–137
10 Jensen P.E.H. & Sottrup-Jensen L. (1986) Primary structure of human α_2-macroglobulin. Complete disulfide bridge assignment and localization of two interchain bridges in the dimeric proteinase binding unit. *J. Biol. Chem.* 261, 15863–15869
11 Lebart L. & Morineau A. (1985) SPAD: Sytème portable pour l'analyse des données. CESIA
12 Liu D., Feinman R.D. & Wang D. (1987) Evidence for active half-molecules of α_2-macroglobulin formed by dissociation in urea. *Biochemistry* 26, 5221–5226
13 Londberg-Holm K., Reed D.L., Roberts D.C., Hebert R.R., Hillman M.C. & Kutney R.M. (1987) Three high molecular weight protease inhibitors of rat plasma. Isolation, characterization and acute phase changes. *J. Biol. Chem.* 262, 438–445
14 Nishigai M., Osada T. & Ikai A. (1985) Structural changes in alpha-2- and ovomacroglobulins studied by gel chromatography and electron microscopy. *Biochim. Biophys. Acta* 831, 236–241
15 Pizzo S.V. & Gonias S.L. (1984) Receptor-mediated protease regulation. In: *Receptors* (P.M. Conn, ed.), Academic Press, Orlando, FL, 1, pp. 177–223
16 Pochon F., Barray M. & Delain E. (1987) Functional α_2-macroglobulin half-molecules induced by cadmium. *Biochem. Biophys. Res. Commun.* 149, 488–492
17 Schramm H.J. & Schramm W. (1982) Computer averaging of single molecules of α_2-macroglobulin and the α_2-macroglobulin/trypsin complex. *Hoppe-Seyler's Z. Physiol. Chem.* 363, 803–812
18 Tapon-Bretaudière J., Bros A., Couture-Tosi E. & Delain E. (1985) Electron microscopy of the conformational changes of α_2-macroglobulin from human plasma. *EMBO J.* 4, 85–89
19 Travis J. & Salvesen G.S. (1983) Human plasma proteinase inhibitors. *Annu. Rev. Biochem.* 52, 655–709
20 Trus B.L. & Steven A.C. (1981) Digital image processing of electron micrographs – the PIC system. *Ultramicroscopy* 6, 383–386
21 Van Heel M. & Frank J. (1981) Use of multivariate statistics in analysing the images of biological macromolecules. *Ultramicroscopy* 6, 187–194
22 Van Leuven F. (1984) Human α_2-macroglobulin. *Mol. Cell. Biochem.* 58, 121–128
23 Van Leuven F., Marynen P., Sottrup-Jensen L., Cassiman J.J. & Van Den Berghe H. (1986) The receptor binding domain of human α_2-macroglobulin. Isolation after limited proteolysis with a bacterial proteinase. *J. Biol. Chem.* 261, 11369–11373
24 Van Leuven F., Marynen P., Cassiman J.J. & Van Den Berghe H. (1988) Proteolysis of human α_2M without hydrolysis of the internal thioesters or expression of the receptor-recognition site. *J. Biol. Chem.* 263, 468–471